ChemCatChem

Research Article
doi.org/10.1002/cctc.202301057

Chemistry Europe
European Chemical Societies Publishing

www.chemcatchem.org

A Mechanistic Study of the Cu-catalyzed *N*-arylation of Hydantoin with Aryl(TMP)iodonium Salts

Linn Neerbye Berntsen[a] and Ainara Nova*[b]

The use of diaryliodonium salts in organic reactions has rapidly increased in the last decade because of their efficiency in arylation reactions. Despite this, mechanistic investigations are still scarce, particularly for copper catalyzed *N*-arylation reactions. Recently, we published the use of the unsymmetrical aryl(TMP)iodonium salts (TMP = 2,4,6-trimethoxyphenyl) for the selective Cu-catalyzed *N*-arylation of hydantoins. In this work, the mechanism of this reaction has been studied by DFT methods, and our results have been compared with previous and new experimental data. In contrast to the mechanism proposed for C–H arylation reactions, our results suggest that deprotonation of hydantoin precedes the oxidative addition of aryl(TMP)iodonium salt, with the oxidative addition to a Cu(I) imido intermediate and ligand rearrangements being the rate-limiting steps. This mechanism agrees with the species observed by NMR spectroscopy, kinetic isotope experiments, and the product yields observed using aryl(TMP)iodonium salts with different steric and electronic properties. In addition, it gives some hints for increasing the efficiency of arylation reactions by tuning the diaryliodonium salt.

Introduction

Diaryliodonium salts have been widely used as electrophilic arylating reagents over the past decade.[1–6] Their usefulness stems from their ability to transfer aryl groups to a range of carbon- and heteroatom nucleophiles, both metal-free[7–12] and transition metal-catalyzed.[13–15] Particularly, the use of copper as transition metal has proven to facilitate the transfer efficiently.[16–26] However, the detailed mechanistic understanding of the copper-catalyzed cross-couplings with diaryliodonium salts is modest and mostly limited to C–H functionalization reactions with symmetrical salts ($Ar_1 = Ar_2$, Scheme 1a).[27–32] While these salts have been extensively used to avoid selectivity issues in arene transfer reactions, unsymmetrical salts ($Ar_1 \neq Ar_2$, Scheme 1b) are preferred when expensive aryl groups are the target, as they allow for the use of a cheaper auxiliary (non-transferred) group (Ar_2 in Scheme1b). In addition, unsymmetrical diaryliodonium salts facilitate tuning of the electronic and steric properties of the auxiliary group to facilitate transfer of the desired arene, which may be needed for the arylation of difficult substrates.

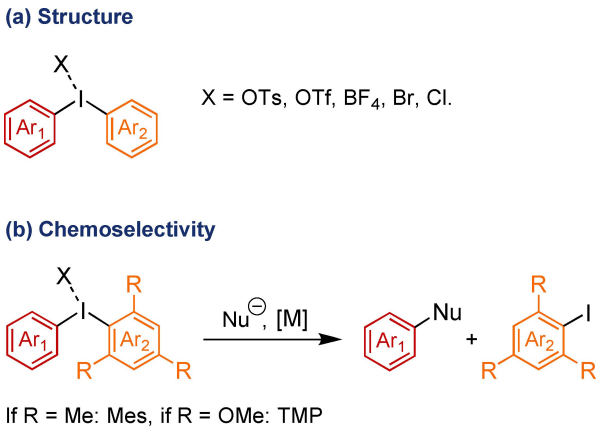

Scheme 1. (a) Structure of diaryliodonium salts. $Ar_1 = Ar_2$ for symmetrical salts, $Ar_1 \neq Ar_2$ for unsymmetrical salts and (b) Chemoselectivity of unsymmetrical salts in metal-catalyzed arylation reactions.

The use of unsymmetrical aryl(Mes)iodonium salts (Mes = mesitylene) for Cu-catalyzed fluorination reactions, have been thoroughly investigated by Sanford and co-workers.[33,34] In their study, a combination of DFT calculations and experiments suggested a Cu(I)/Cu(III)-catalytic cycle, starting with the oxidative addition of the aryl(Mes)iodonium salt. This step is also assumed to be the first in the few computational studies of Cu-catalyzed C–H arylation reactions with diaryliodonium salts.[30–32] Closely related to the aryl(Mes)iodonium salts are the aryl(TMP)iodonium salts (TMP = 2,4,6-trimethoxyphenyl). Recent interests in the use of aryl(TMP)iodonium salts can be attributed to their excellent selectivity in aryl transfer reactions with various nucleophiles.[8,35–41] As far as the authors are concerned,

[a] *Dr. L. Neerbye Berntsen*
Department of Chemistry
University of Oslo
P.O. Box 1033 Blindern
N-0315 Oslo (Norway)

[b] *Dr. A. Nova*
Hylleraas Centre for Quantum Molecular Sciences and Centre for Materials Science and Nanotechnology
Department of Chemistry
University of Oslo
P.O. Box 1033 Blindern
N-0315 Oslo (Norway)
E-mail: a.n.flores@kjemi.uio.no
Homepage: http://www.uiocompcat.info/ainaranova

Supporting information for this article is available on the WWW under https://doi.org/10.1002/cctc.202301057

no mechanistic investigation of Cu-catalyzed arylation using aryl(TMP)iodonium salts have been reported.

Our group have recently developed a regioselective Cu-catalyzed N^3-arylation of hydantoins using unsymmetrical diaryliodonium salts in the presence of triethylamine.[42] A copper(II) nitrate salt facilitates the selective transfer of several aryl groups from [Ar(TMP)I]OTs to the N^3-position in the hydantoins generating N^3-arylated hydantoins and TMP-I as a byproduct. Similar strategies have been used for the *N*-arylation of weak *N*-nucleophiles.[21,23–25,43,44] The absence of previous mechanistic studies for these reactions made us propose two different reaction mechanisms, both based on a Cu(I)/Cu(III) catalytic cycle (Scheme 2). In pathway I, the imide NH-group is deprotonated by a Cu(I)-species prior to the oxidative addition of the diaryliodonium salt. This mechanism has been proposed for Ullman-type C–N bond coupling reactions using aryl iodides.[45,46] In pathway II, the oxidative addition of the diaryliodonium salt is the first step followed by the deprotonation, which is the mechanism proposed for C–H arylation reactions with diaryliodonium salts.[16] In both pathways, the final product is formed by reductive elimination of a Cu(III)-species.

In this work, the two mechanisms represented in Scheme 2 have been explored using DFT calculations. The non-catalyzed deprotonation of hydantoin by the amine was also considered. Special efforts were made to explain the chemo- and regioselectivity of the reaction and to support the computational results with previous experimental observations and new experimental work.

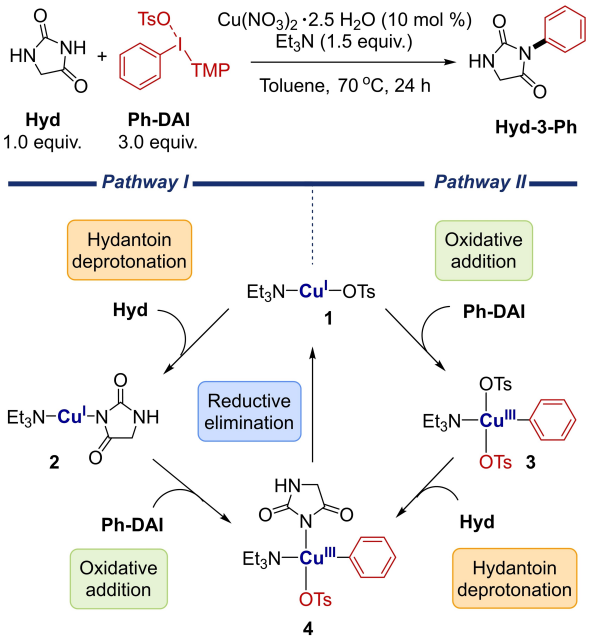

Scheme 2. Proposed Cu(I)/Cu(III) catalytic cycles for the N^3-arylation of hydantoins.

Results and discussion

The two mechanisms depicted in Scheme 2 were studied by using DFT calculations (PBE0-D3/def2TZVP/CPCM//PBE0-D3/def2SVP/CPCM), see Supporting Information for details.[47–49] Free energies were obtained considering standard state conditions. The reactants selected to study the full mechanism were hydantoin (**Hyd**) and [Ar(TMP)I]OTs with Ar = Ph (**Ph-DAI**). The influence of other aryl groups in the diaryliodonium salts was studied for the selected mechanism (Pathway 1).

Before starting the study of the catalytic cycle, we looked at the reaction thermodynamics. The optimal reaction conditions requires an excess of [Ph(TMP)I]OTs and triethylamine base (TEA). The poor solubility of [Ph(TMP)I]OTs can contribute to the need for 3 equivalents of this salt (*vide infra*). The 1.5 equivalents of TEA allows the amine to act as catalyst ligand and base driving the Hyd deprotonation step. Including the amine in the reaction equation (Scheme 3), the arylation of Hyd in the N^1 and N^3 positions are highly exergonic by 56.7 and 54.9 kcal/mol, respectively. The small thermodynamic preference for the N^1-arylation compared to the N^3-arylation indicates that the selective formation of the N^3-arylated product **Hyd-3-Ph** is due to kinetic preferences. In the absence of amine, TsOH would be formed and made the reaction thermodynamics less favored ($\Delta G = -40.3$ and -38.5 kcal/mol for the N^1 and N^3, respectively). The lack of reactivity in the presence of a base (NaH) and absence of amine, supports the role of amine as Cu-ligand.[42] TEA could also be responsible for the reduction of $Cu(II)(NO_3)_2$ to (TEA)Cu(I)(OTs) (**1** in Scheme 2) as suggests the instant color change of the solution containing copper upon

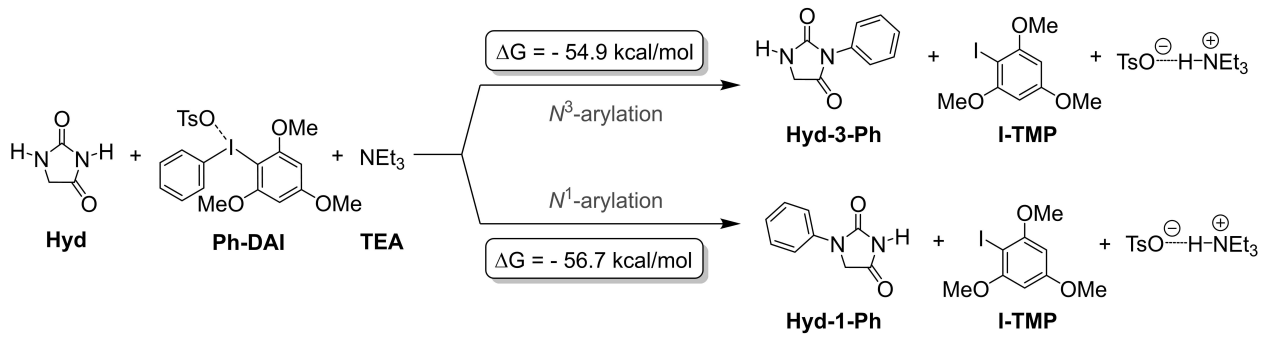

Scheme 3. Calculated free energies (in kcal/mol) for the N^1- and N^3-arylation of hydantoins (Hyd) with phenyl(TMP)iodonium salt (**Ph-DAI**) and triethylamine (TEA) acting as a base.

addition of TEA.[50] Diamagnetic Cu(I) and Cu(III) intermediates are expected because the reaction can be followed by ^{1}H NMR spectroscopy (see Figure S5). We used OTs^- instead of NO_3^- anion to charge balance the Cu(I) complex because of its higher concentration in solution. In addition, OTs was found to give the best reaction yields when compared with other counter anions (Table S1). All species considered in the catalytic cycle were neutral or treated as ion pairs because of the low polarity of toluene.

Before analyzing **Pathway I** and **II**, we evaluated the deprotonation of Hyd by TEA in the absence of Cu. The deprotonation of both N^1 and N^3 protons was found to be endergonic with energies ranging from 6.9 to 11.0 kcal/mol (**Hyd-32(34, 12)-TEA** in Scheme 4). In all cases, the ion pairs formed are stabilized by H-bond interactions between the nitrogen anion of Hyd and the C–H groups of TEA and between the N–H and C=O groups. The transition state with the lowest energy involves the deprotonation of the N^3 proton (the most acid proton, **TSHyd-32** in Scheme 3) assisted by the C=O group in 2 position, and has an energy of 9.7 kcal/mol. This energy is 5.7 kcal/mol more favorable than the energy barrier to deprotonate the N^1 position, which could account for the selectivity observed. Overall, while endergonic, deprotonation reactions in N^1 and N^3 positions are kinetically accessible at the experimental conditions (70 °C) and should be considered.

Pathway I

The Cu(I) catalyzed deprotonation of hydantoins is the first reaction in Pathway 1. This process involves two steps: (1) the coordination of Hyd to Cu(I) and (2) the cleavage of the N–H interaction by OTs assisted by the hydantoin carbonyl group in 2 position. With the N^3 site, these steps have similar energy barriers of 6.8 and 7.1 kcal/mol with deprotonation taking place concurrently to Hyd coordination (in **TS5-6**). In contrast, with N^1, deprotonation takes place in the second step, which has the highest energy barrier (**TS6-7-N1** = 12.4 kcal/mol). In both cases, the deprotonation of TsOH by TEA, **7** (**7-*N1***)→**9** (**9-N1**), makes the overall process exergonic by 12.5 kcal/mol for the N^3-product and 7.4 kcal/mol for the N^1-product (**9-N1** is shown in Scheme S3). Comparing the Cu-assisted (in Scheme 5) with the TEA-assisted (in Scheme 4) deprotonation pathways, the former is preferred by ca. 3 kcal/mol. However, the lower concentration of Cu compared to TEA, and the relatively low energy barriers, may allow both processes to take place. Nevertheless, the deprotonation of Hyd is only exergonic when the deprotonated Hyd bonds to Cu yielding intermediates **2** and **9** in Figure 1. These intermediates are thermodynamically more preferred than **2-N1** and **9-N1** consistently with the product selectivity observed. The formation of other reaction intermediates by coordination of an additional TEA to Cu(I) (**8** and **10**) or by changing the coordination site of Hyd from N^3 to O^2 in **6** (Scheme S3) were also considered, but, although relatively stable, they are not involved in the rate limiting pathway.

The oxidative addition of [Ph(TMP)I]OTs to **2** is the following reaction step. Both Ph–I and TMP–I bond cleavage were considered. Interestingly while the interaction of Cu(I) with TMP in **11-TMP** is more favorable than with Ph in **11** by 2.2 kcal/mol, the oxidative addition of the PhI is thermodynamically preferred to that of the TMP–I by 11.5 kcal/mol (**12** and **12-TMP** in Scheme 6). The long Cu–C distances between Ph and TMP in **11** and **11-TMP** (3.15 and 4.06 Å, respectively) suggests that there is no coordination between Cu and the aryl groups but rather

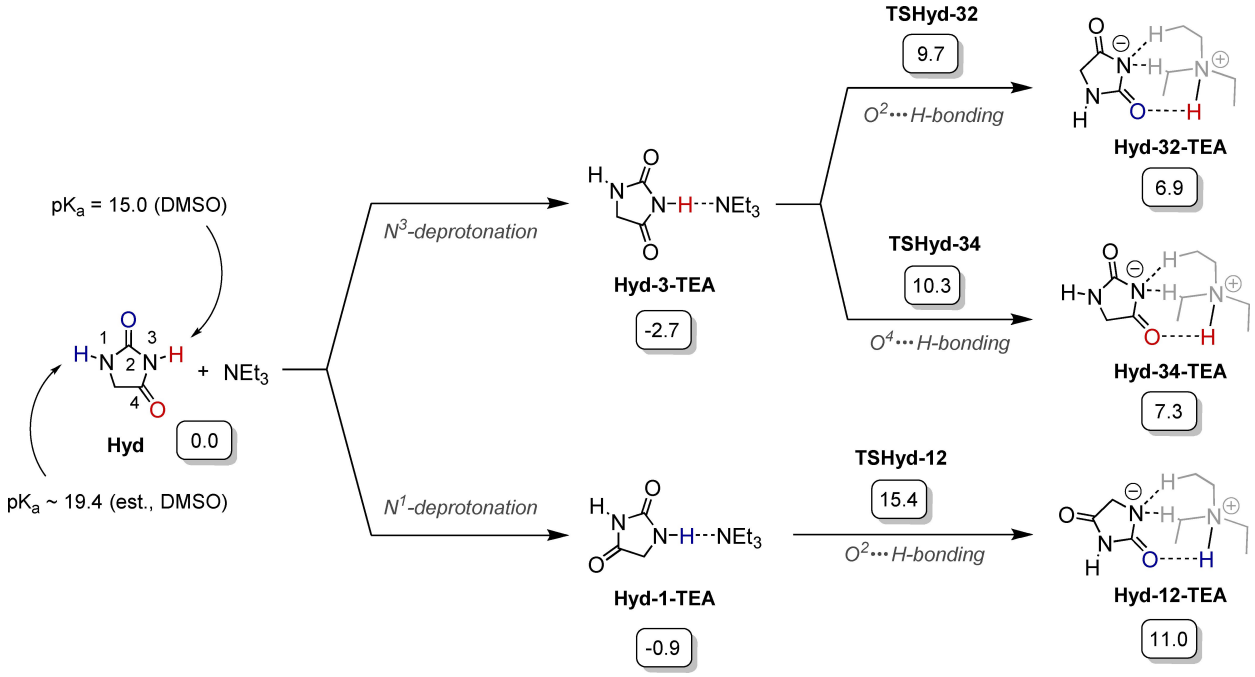

Scheme 4. Calculated free energies (in kcal/mol) for the N^3 and N^1 deprotonation of Hyd with TEA. Energies over the arrows correspond to transition states. Reference for pK_a-values: N3[51] and N1.[52]

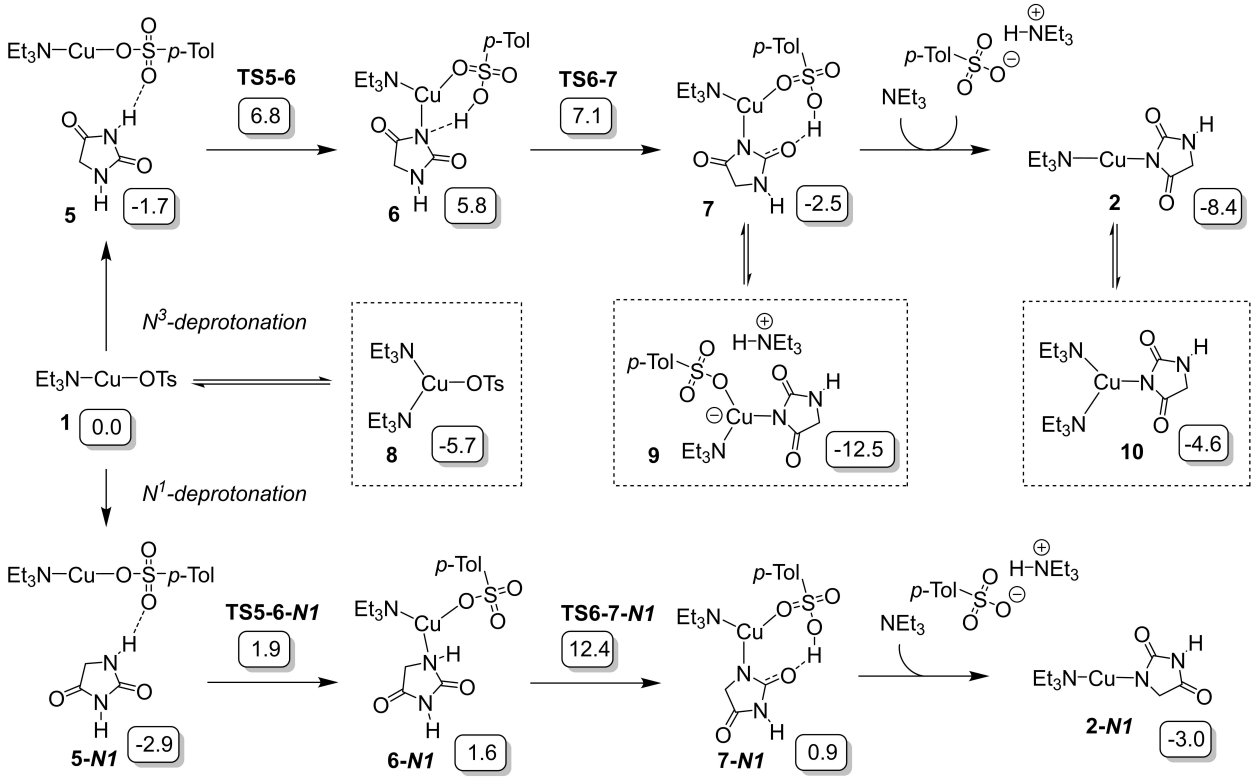

Scheme 5. Free energies (in kcal/mol) for the N^1- and N^3 deprotonation of Hyd with **1**. Energies over the arrows correspond to transition states. Off cycle species in dashed squares.

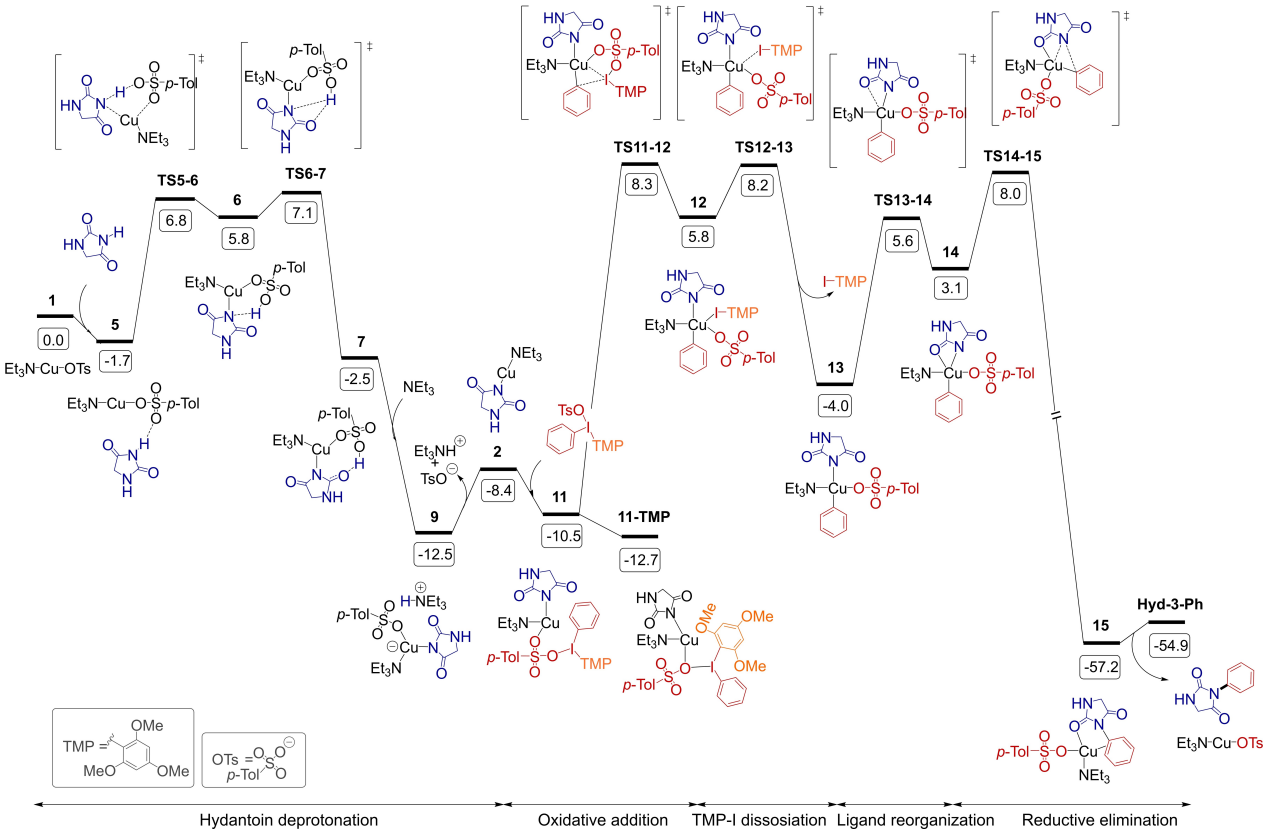

Figure 1. Free energy profile (in kcal/mol) for Pathway I.

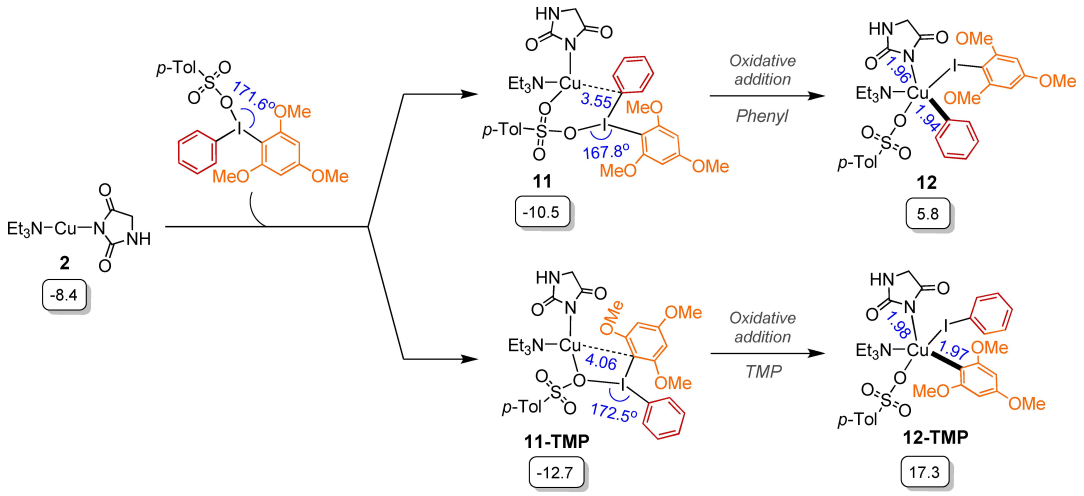

Scheme 6. Free energies (in kcal/mol) for the oxidative addition of phenyl(TMP)iodonium tosylate **Ph-DAI** to **2** by the Ph(C)-I and TMP(C)-I bonds. Energies are in kcal/mol. Selected angles (in °) and distances (in Å) in blue.

Van der Waal interactions. The angle between TMP and OTs are also significantly different in **11** and **11-TMP** (167.8° and 79.6°, respectively). However, this difference should not explain the lower energy of **11-TMP** since the most preferred conformation of **Ph-DAI** has a TMP–Cu–OTs angle closer to **11** (171.6°). On the other hand, the longer Cu–C(Ar) bond distance in **12-TMP** than in **12** (1.97 and 1.94 Å, respectively) and the higher congestion around Cu in **12-TMP** suggest that steric hindrance plays a main role in destabilizing **12-TMP** compared to **12**. This intermediate has a square-pyramidal molecular geometry with OTs in the apical position. The large energy preference for **12** compared to **12-TMP** accounts for the 100% chemoselectivity observed in the arylation of **Hyd** with **Ph-DAI**.

The energy profile for **Pathway I**, including all reaction steps for the formation of **Hyd-3Ph**, is shown in Figure 1. After the formation of **11**, the oxidative addition is a two-step process that goes via the Cu(III) pentacoordinate intermediate **12**. The transition state with the highest energy is **TS11-12** and involves the C–I bond cleavage. This transition state is 16.7 kcal/mol above intermediate **2** and 21.0 kcal/mol above **11-TMP**. The product of the oxidative addition (**13**) has the Hyd and Ph groups *trans* to each other. Indeed, we could not find an intermediate with the two groups in a *cis* arrangement (**4** in Scheme 2) because of a barrierless reductive elimination. However, a ligand reorganization pathway involving a penta-coordinated Cu(III) complex (**14**) was found to connect intermediate **13** with the reductive elimination product **15**, in which **Hyd-3-Ph** bonds to Cu(I) by the Ph and C^4-carbonyl group. The energy barrier of this process is 12.0 kcal/mol taking intermediate **13** as energy reference, with the C–N bond coupling TS (**TS14–15**) being the one with the highest energy.

Overall, **Pathway I** has the three main steps represented in Scheme 2 (Hyd deprotonation, oxidative addition and reductive elimination) with the only difference that intermediate **4** has the two substituents *trans* to each other (**13** in Figure 1). Deprotonation of Hyd has a low energy barrier and is highly exergonic thanks to its coordination to **1** and formation of a Cu(I)-tricoordinated ion pair with $[TEAH]^+$ (**9**). This step is followed by an endergonic oxidative addition, which has the highest energy barrier of the overall process ($\Delta G = 21.0$ kcal/mol). Finally, the reductive elimination of **Hyd-3-Ph** is the irreversible step that drives the reaction towards the final product. Even though, for **Ph-DAI**, the oxidative addition transition state (**TS11-12** = 8.3 kcal/mol) has the highest energy, the dissociation of I-TMP (**TS12-13** = 8.2 kcal/mol) and reductive elimination (**TS14-15** = 8.0 kcal/mol) transition states are very close in energy indicating that the rate-limiting step may change by changing the diaryliodonium salt substrate. Indeed, the nonlinear trend in yields observed using electron-donating and -withdrawing aryl substituents in the diaryliodonium salt is consistent with a change in the rate-limiting step when going to the extremes (*vide infra* for details). In addition, the highest impact in yield observed by changing the **DAI-** compared to the **Hyd**-substituents[42] is consistent with the diaryliodonium salt being involved in the rate-limiting step. The overall energy barrier (or reaction energy span)[53] of 21.0 kcal/mol seems too low for a reaction that needs 70 °C to proceed. However, temperature is probably required to increase the concentration of catalyst and reactants in solution. To prove this assumption, we tested the reaction in DMSO where all reactants were soluble (see Table 1). The arylation reaction was completed in less than 1.5 hours at 70 °C with only 1.5 equivalents of **Ph-DAI** (with 76% yield, entry 3), while it took up to 24 hours at the same temperature in toluene (78% yield, entry 1). In addition, 17% yield was obtained after 1 day of reaction in DMSO at room temperature in contrast to the lack of reactivity observed in toluene (entries 4 and 2). Yields ranging from 75–78% were the maximum achieved under these conditions. As reported in our original communication,[42] trace amounts of the *N*,*N*-bisarylated product was observed as a byproduct in the reaction, which prevents the use of a larger concentration of TEA required to achieving full conversion. In the DMSO-reaction (entry 3), around 8% bis-arylated product was observed, and

Table 1. Control reactions.[a]

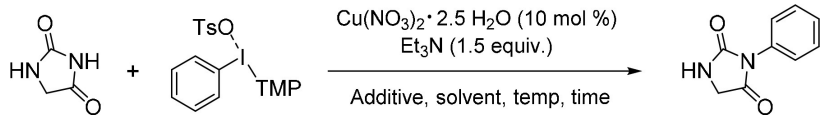

Entry	[Ph(TMP)I]OTs (equiv.)	Solvent	Temp (°C)	Time (h)	Yield (%)[a]
1	3.0	Toluene	70	24	78[b]
2	3.0	Toluene	25	24	nr
3	1.5	DMSO	70	1.5	76
4	3.0	DMSO	25	24	17
5	3.0	DMSO	25	96	75

[a] Conditions: Hydantoin **Hyd** (0.2 mmol, 1.0 equiv.), [Ph(TMP)I]OTs **Ph-DAI** (as specified.), $Cu(NO_3)_2 \cdot 2.5\ H_2O$ (0.02 mmol, 0,.1 equiv.), Et_3N (0.3 mmol, 1.5 equiv.) in solvent (2 mL) as specified. [a] ^1H NMR yield using mesitylene as internal standard. [b] Isolated yield.

the remaining 16% was unconverted starting material (**Hyd**) (see supporting info for further details).

The reaction was also monitored by ^1H NMR spectroscopy in DMSO-d_6 to identify reaction intermediates (see supporting information). Figures S5, S7 and S8 show the simultaneous formation of **Hyd-3-Ph**, I-TMP and protonated TEA-species in a similar amount, without any reservoir effect. This result is in agreement with the low energy barriers obtained for the oxidative addition and reductive elimination steps, which prevents the accumulation of intermediate **9** and protonated TEA.

Pathway II

The oxidative addition of **Ph-DAI** to complex **1** is the first step in **Pathway II** (Scheme 7). The coordination of this species to Cu(I) (**16**) is exergonic by 5.0 kcal/mol. Attempts to get the oxidative addition transition state from intermediate **16** were unsuccessful. This would have led to a pentacoordinated Cu(III) complex containing two OTs anions with high steric hindrance. Still, we found an oxidative addition transition state from intermediate **17**, in which TEA has been dissociated. Even though the energy for this step (**TS17-18** = 13.2 kcal/mol) is feasible at the experimental conditions, it is 4.9 kcal/mol higher than the oxidative addition of **Ph-DAI** to **11** in Pathway I. The

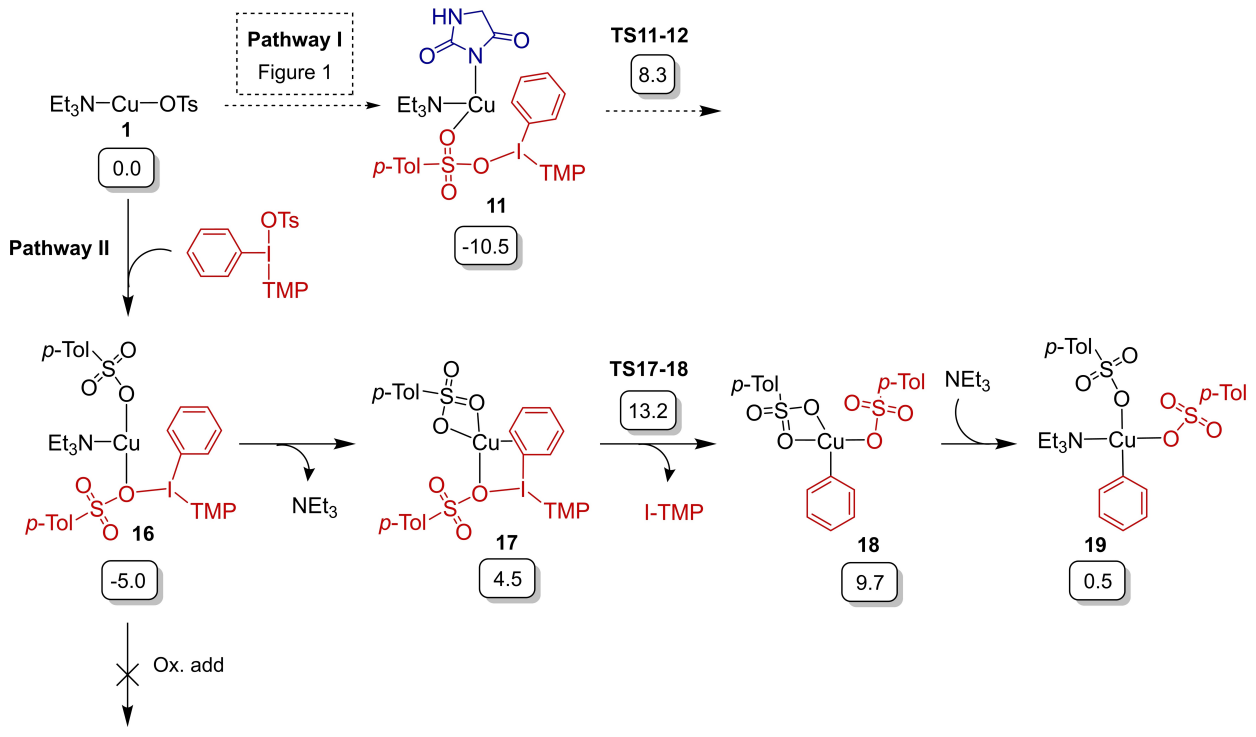

Scheme 7. Free energies (in kcal/mol) for oxidative addition of [Ph(TMP)I]OTs to **1**, which is the first step for Pathway II. Energies over the arrows correspond to transition states.

lowest energy of Pathway I can be related with the stability of Cu(I) intermediates provided by imido ligands, which is shown by the energy difference between intermediate **11** and **16** ($\Delta G = 5.5$ kcal/mol in favor of **11**). Cu(I) imido intermediates have also been shown to participate in the Ullmann reaction.[54] These results suggest that Pathway I is preferred over Pathway II (see Figure S11). For completeness, we looked at the deprotonation of Hyd from intermediate **19** (see Scheme S4). This reaction gives an energy barrier for the deprotonation of the N^3 position of 14.9 kcal/mol (**TS21-22**), which is higher than the energy barrier obtained with TEA as base in the absence of copper (see Scheme 4). Therefore, a base-assisted deprotonation of **Hyd** followed by OTs-by-Hyd anion exchange process from intermediate **19** is preferred in Pathway II. Finally, a transition state for reductive elimination was found at an energy of 5.2 kcal/mol (**TS22-23** in Scheme S4).

Influence of aryl-substituents in the oxidative addition barriers and reaction yields

In our original communication we reported a broad scope of reactions with various aryl(TMP)iodonium tosylates. The variety in product yields stemming from substituted aryl-groups clearly indicated the presence of substituent effects. For instance, we found that salts bearing an electron withdrawing nitro group in the *para*-position (**No-DAI**), gave a reduction in product yield of almost 20% compared to the neutral **Ph-DAI**. This result is consistent with previous observation using unsymmetrical diaryliodonium salts, in which the more electron-rich or the least bulky arene is usually transferred.[15,33,34] Unexpectedly, the electron-rich dihydrobenzofuran (**Bf-DAI**) gave only 30% of the desired product **Hyd-3-Bf**. The sterically hindered *ortho*-methylated salt (**To-DAI**) was ineffective in the arene transfer and no **Hyd-3-To** was afforded. To evaluate whether the trends in yield correlate with the energy barriers for Pathway I, the energy profiles for the oxidative addition and reductive elimination steps were computed with **No-**, **Bf-** and **To-DAI** (see Figure 2).

This study shows that the electronic and steric difference of **Ph-**, **No-**, **Bf-** and **To-** groups are sufficient to change the rate-determining step of the reaction. While the TS with the highest energy for Ph is the oxidative addition (**TS11-12**), it is the I-TMP dissociation (**TS12-13**) with **No-DAI**, and the reductive elimination (**TS14-15**) with **Bf-** and **To-DAI** substrates. It seems that electron-withdrawing groups disfavors the release of the I-TMP, while electron-donors and sterically hindered substituents disfavors all Cu(III) intermediates including the corresponding TSs. The latter may be caused by the strong electron-donation of both imido and aryl groups, which are *trans* to each other. The longer the Cu–N and Cu-(C)Ar bonds in intermediate **13** (1.964 and 1.925 Å with **Ph**, 1.952 and 1.921 Å with **No**, 1.966 and 1.925 Å with **Bf**, and 1.974 and 1.945 Å with **To**, respectively) the lower the stability. The most stable intermediate (catalyst resting state) also changes from **11-TMP** to **9** when going from **Ph, No and To** to **Bf** aryl groups. Accordingly, the overall energy spans for **Ph-**, **No-**, **Bf-** and **To-DAIs** are 21.0, 21.3, 22.1, and 27.5 kcal/mol, which are in qualitative agreement with the yields obtained with these substrates (78%, 59%, 30% and 0% yield, respectively).

To further support the computational results, we synthetized d_5-[Ph(TMP)I]OTs **PhD-DAI** to perform deuterium-labelling experiments. Using this substrate under standard conditions yields the deuterated product (**Hyd-3-PhD**) in 44% yield (Scheme 8). In addition, a KIE of 1.31 was obtained by using parallel experiments with **PhD-** and **Ph-DAI** as substrates (see Supporting Information). The distance from the deuterated site(s) to the location of the bond-breaking in the rate-limiting step (oxidative addition) indicates a β-secondary effect. The use of **PhD-DAI** in intermediate **11-TMP** and **TS11-12** leads to a slight increase in the energy barrier of 0.1 kcal/mol, consistent with a KIE of 1.18 (see Figure S12). Further, considering **11** as the resting state, the energy span increases to 0.2, which corresponds to a KIE of 1.34. Both results show a good agreement with the experimental KIE-value of 1.31.

Conclusions

In this work, the mechanism for the N^3-arylation of hydantoin using aryl(TMP)iodonium salts (TMP = 2,4,6-trimethoxyphenyl) has been studied with DFT methods, and Figure 3 summarizes our results. We found that the preferred pathway consists of an initial deprotonation of hydantoin by the triethylamine base (TEA). This reaction yields the formation of the Cu(I)-imido intermediate **2** via two kinetically accessible pathways: (1) the organic deprotonation by TEA and (2) the Cu(I) assisted deprotonation by OTs anion. In both cases, the carbonyl groups of the substrate participate in the reaction by stabilizing the abstracted proton. Deprotonation of hydantoin is followed by the coordination of the aryl(TMP)iodonium salt. Despite transferring TMP to Cu being thermodynamically unfavored, we found that TMP may interact with Cu more strongly than other aryl substituents, yielding **11-TMP**. Although this species is an off-cycle intermediate in equilibrium with **11**, it is relevant because it may behave as the catalyst resting state.

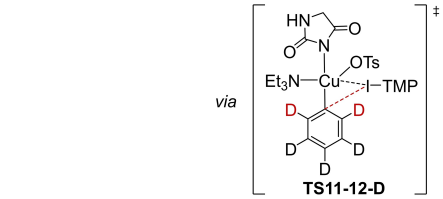

Scheme 8. Reaction conditions for deuterium-labeling experiment with isolated yields. [a] ^{1}H NMR yield measured from the crude reaction mixture (in parenthesis). Schematic representation of the oxidative addition transition state showing the deuteration sites in closest proximity to the bond-breaking site, marked in red.

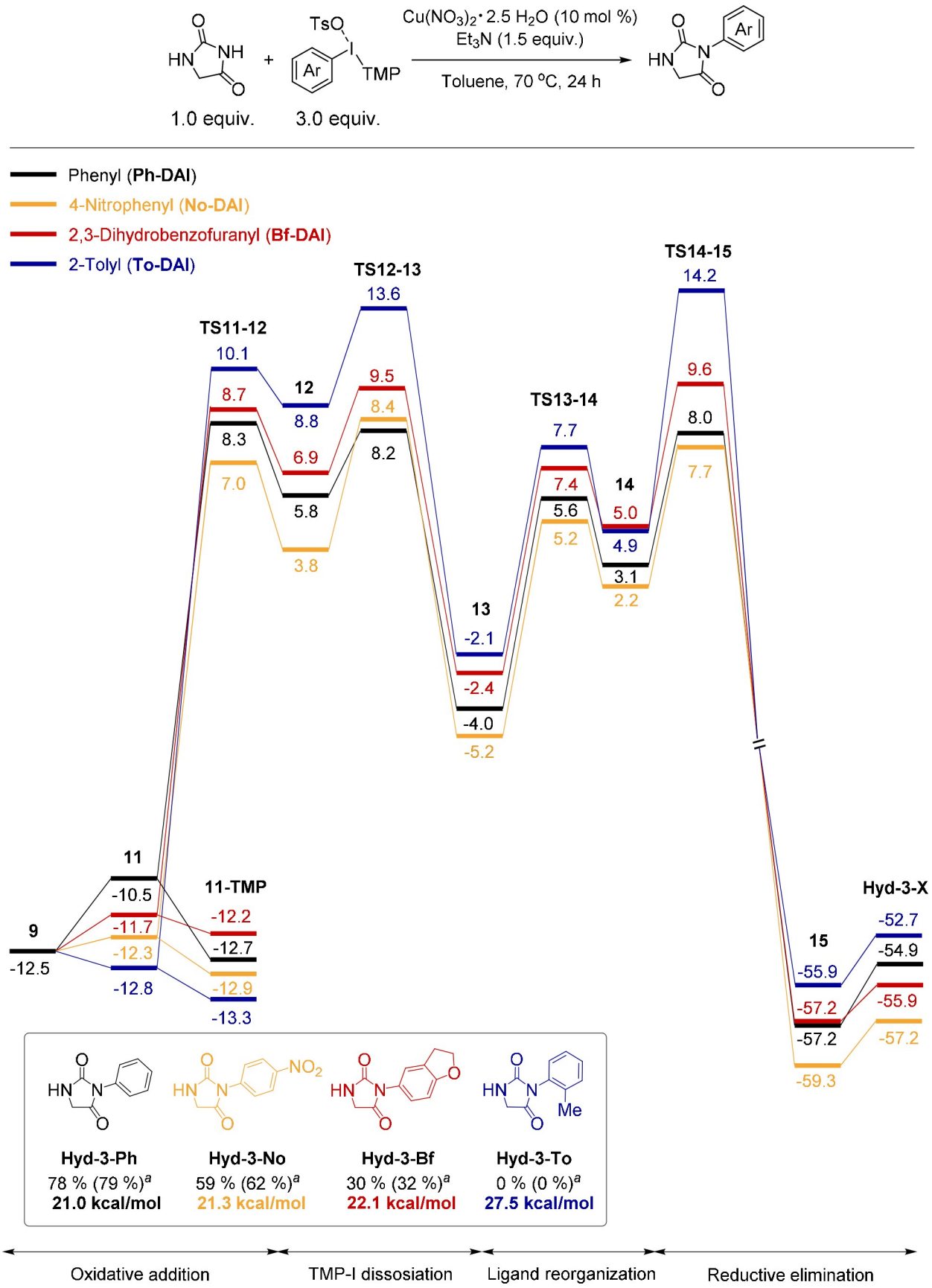

Figure 2. Free energies profile (in kcal/mol) for the oxidative addition of aryl(TMP)iodonium tosylates to 9 following Pathway I. Energy span (highest TS energy – 11-TMP) and reaction yields are given for each substrate (see scheme for reaction conditions).[a] ^{1}H NMR yield measured from the crude reaction mixture (in parenthesis).

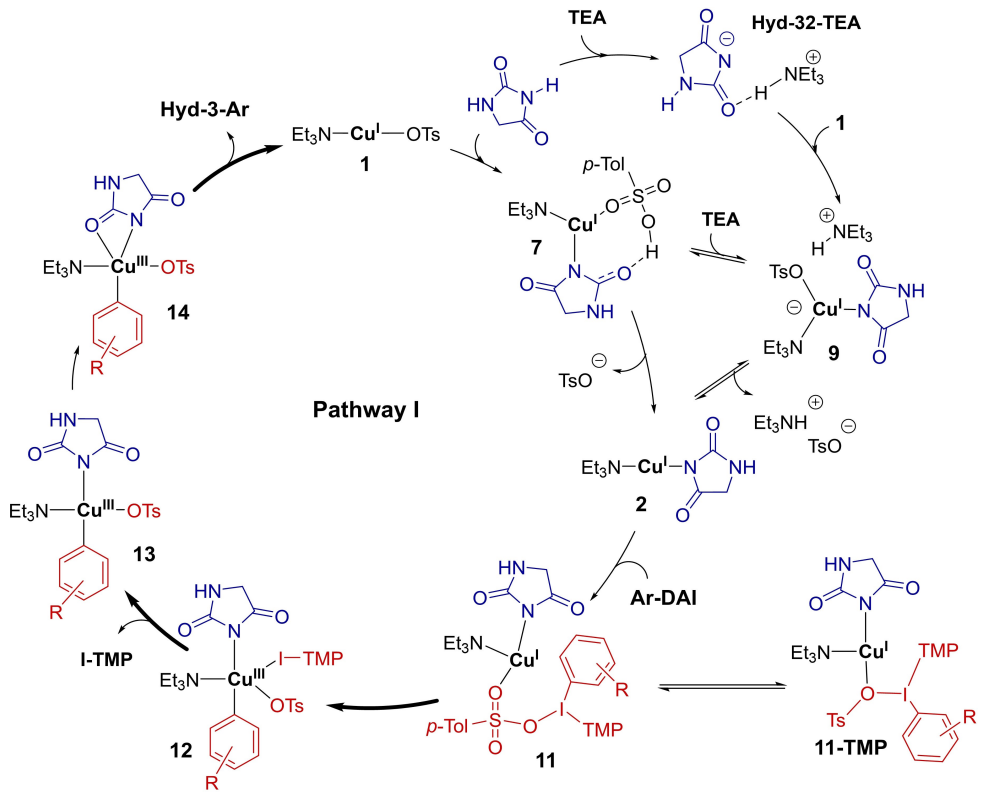

Figure 3. Proposed catalytic cycle for the regio- and chemoselective N^3-arylation of hydantoins (Pathway I).

The oxidative addition of [Ar(TMP)I]IOTs in **11** yields the pentacoordinate Cu(III) intermediate **12**, in which the imido and aryl substituents are *trans* to each other. Therefore, following I-TMP dissociation, imido and aryl ligands must relocate in a *cis* arrangement for reductive elimination of the final product (**Hyd-3-Ar**). This isomerization process goes via the Cu(III) pentacoordinate intermediate **14**, where both imido and carbonyl groups of hydantoin interact with Cu.

We found that three steps are susceptible to being rate-limiting: the oxidative addition of **Ar-DAI**, the decoordination of I-TMP and the ligand reorganization required for the reductive elimination step (steps with bold arrows). Similarly, three species may behave as catalyst resting states: **9**, **11** and **11-TMP**, depending on the concentration of TEA and **Ar-DAI** and the electronic and steric properties of the **Ar-DAI**. This result explains the absence of a trend when using substrates with electron-donating and electron-withdrawing properties. In addition, it supports the idea that both aryl groups in diaryliodonium salts should be optimized to achieve the highest activity in arylation reactions. Although this work is based on the functionalization of hydantoin, the results herein should apply to other substrates with imide functionalities.

Experimental Section

Commercially available reagents and solvents were purchased from Sigma-Aldrich and TCI and used without further purification unless stated otherwise. Thin layer chromatography was performed on 60 F254 silica coated aluminum plates from Merck and visualized using UV-light or KMnO4-stain. Flash chromatography was performed on silica gel from Merck (Silicagel 60, 40–63 μm) using Isco Inc. CombiFlash Companion with PeakTrack software (v.1.4.10). 1H- and 13 C-NMR spectra were recorded either using Bruker DPX300, DRX500, AVI600 or AVII600 spectrometers. Spectra were calibrated using the residual solvent peaks for DMSO-d6 (1H: 2.50 ppm; 13 C: 39.52 ppm) and CD3CN (1H: 1.94 ppm; 13 C: 1.32/118.26 ppm). All spectra were recorded at 298 K unless otherwise stated. High-resolution mass spectra (HRMS) were obtained by electron spray ionization (ESI) on Bruker Daltonik GmbH MAXIS II ETD spectrometer. All non-deuterated arylated hydantoins and diaryliodonium salts were reported in our previous work.[42]

Synthesis of Phenyl-d5-(2,4,6-trimethoxyphenyl)iodonium tosylate (PhD-DAI): Following a literature procedure,[35] iodobenzene-d_5 (2.00 mmol, 1.00 equiv.) and acetonitrile (2 mL) were added to a 25 mL round-bottom flask and equipped with a magnetic stir bar. *p*-Toluenesulfonic acid monohydrate ($TsOH \cdot H_2O$) (2.02 mmol, 1.01 equiv.) was added in one portion at room temperature, followed by *m*-chloroperbenzoic acid (*m*CPBA) 2.02 mmol, 1.01 equiv.). The flask was lowered into a pre-heated heating block set at 77 °C, and stirred for 30 minutes. 1,3,5-trimethoxybenzene (TMP–H) (2.02 mmol, 1.01 equiv.) was then added and the resulting solution was stirred for 5 minutes at 77 °C. The flask was cooled to ambient temperature before acetonitrile was removed under reduced pressure. The resulting crude oil was triturated with diethyl ether (20 mL). The precipitate was isolated by vacuum filtration with a fritted funnel and rinsed with diethyl ether (3×10 mL), then further dried under high vacuum. The process afforded **PhD-DAI** as a pale pink powder (1.10 g, 87 %). ^{1}H NMR (600 MHz, DMSO-d_6): δ 7.47 (d, J = 8.0 Hz, 2H), 7.10 (d, J = 7.8 Hz, 2H), 6.47 (s, 2H), 3.94 (s, 6H), 3.87 (s, 3H), 2.28 (s, 3H). ^{13}C NMR (151 MHz, DMSO-d_6): δ 166.2,

159.4, 145.8, 137.6, 133.9 (t, $J=25.7$ Hz), 131.1 (t, $J=24.5$ Hz), 128.0, 125.5, 115.8, 92.1, 87.0, 57.3, 56.2, 20.8. HRMS (ESI) m/z $[M–OTs]^+$: Calcd. for $C_{15}H_{11}D_5INO_3^+$: 376.0453, found: 376.0452.

Synthesis of 3-Phenyl-d5-hydantoin (Hyd-3-PhD): Following our own procedure,[42] Hydantoin (0.2 mmol, 1.0 equiv.), phenyl-d_5-(TMP)iodonium tosylate **PhD-DAI** (0.6 mmol, 3.0 equiv.) and $Cu(NO_3)_2 \cdot 2.5\ H_2O$ (4.7 mg, 0.02 mmol, 0.1 equiv.) were added to a 7 mL screw cap vial equipped with a magnetic stir bar. Toluene (2 mL) was added and the vial was placed in a pre-heated vial insert heating block set to 70 °C. Triethylamine (42 μL, 0.3 mmol, 1.5 equiv.) was added via a syringe, and the suspension was stirred for 24 hours at 70 °C. The resulting mixture was allowed to cool to room temperature before it was concentrated under reduced pressure. The crude mixture was purified by column chromatography using gradient elution (SiO_2, hexane:acetone [90:10%→80:20%→70:30%]) which gave **Hyd-3-PhD** as colorless solid (15.9 mg, 44%). ^{1}H NMR (600 MHz, CD_3CN): δ 6.23 (br s, 1H), 3.99 (d, $J=1.3$ Hz, 2H). ^{13}C NMR (151 MHz, CD_3CN): δ 172.0, 157.9, 133.3, 129.4 (t, $J_{C-D}=24.7$ Hz), 128.5 (t, $J_{C-D}=24.6$ Hz), 127.4 (t, $J_{C-D}=25.0$ Hz), 47.2. HRMS (ESI) m/z $[M+Na]^+$: Calcd. for $C_9H_3D_5N_2NaO_2^+$: 204.0792, found: 204.0792.

Supporting Information

The authors have cited additional references within the Supporting Information.[55-60]

The following files are available free of charge: Experimental details, synthetic procedures, ^{1}H NMR reaction monitoring, computational details, supporting schemes for pathway I and II, ^{1}H and ^{13}C NMR spectra (PDF). Optimized geometries of all energy minima (reactants, intermediates, and products) and saddle points (transition states) (XYZ)

Author Contributions

The manuscript was written through contributions of all authors. All authors have given approval to the final version of the manuscript.

Acknowledgements

L.N.B. gratefully acknowledges the Department of Chemistry at the University of Oslo for funding her Ph.D. fellowship. The project has received support from UiO: Life Science, the Research Council of Norway through the Norwegian NMR Platform, NNP (226244/F50), and the Norwegian Metacenter for Computational Science (NOTUR) for computational resources (No. nn4654k). A.N. acknowledge the support from the Research Council of Norway through the Centre of Excellence (No. 262695) and its FRINATEK program (No. 314321). We want to acknowledge Alexander Sandtorv for initiating the project and provide experimental insight in the reaction, and Julie Heron for her contribution to locate some of the intermediates.

Conflict of Interests

The authors declare no conflict of interest.

Data Availability Statement

The data that support the findings of this study are available in the supplementary material of this article.

Keywords: copper · catalysis · density functional theory · Hydantoin · N-Arylation · reaction mechanisms

[1] E. A. Merritt, B. Olofsson, *Angew. Chem. Int. Ed.* **2009**, *48(48)*, 9052–9070.
[2] Y. Wang, G. An, L. Wang, J. Han, *Curr. Org. Chem.* **2020**, *24(18)*, 2070–2105.
[3] N. R. Deprez, M. S. Sanford, *Inorg. Chem.* **2007**, *46(6)*, 1924–1935.
[4] M. S. Yusubov, A. V. Maskaev, V. V. Zhdankin, *Arkivoc* **2011**, *2011(1)*, 370–409.
[5] Z. Novák, K. Aradi, B. Tóth, G. Tolnai, *Synlett* **2016**, *27(10)*, 1456–1485.
[6] B. Olofsson, In *Hypervalent Iodine Chemistry*, Wirth, T. Ed.; Springer: Cham, **2016**, pp 135–166.
[7] N. Jalalian, E. E. Ishikawa, L. F. Silva, B. Olofsson, *Org. Lett.* **2011**, *13(6)*, 1552–1555.
[8] S. Basu, A. H. Sandtorv, D. R. Stuart, D. R. Beilstein, *J. Org. Chem.* **2018**, *14*, 1034–1038.
[9] G. Kervefors, L. Kersting, B. Olofsson, *Chem. Eur. J.* **2021**, *27(18)*, 5790–5795.
[10] P. Villo, G. Kervefors, B. Olofsson, *Chem. Commun.* **2018**, *54(64)*, 8810–8813.
[11] L. Chan, A. McNally, Q. Y. Toh, A. Mendoza, M. J. Gaunt, *Chem. Sci.* **2015**, *6(2)*, 1277–1281.
[12] Y. Chen, Y. Gu, H. Meng, Q. Shao, Z. Xu, W. Bao, Y. Gu, X.-S. Xue, Y. Zhao, *Angew. Chem. Int. Ed.* **2022**, *61(28)*, e202201240.
[13] Z. Huang, Q. P. Sam, G. Dong, *Chem. Sci.* **2015**, *6(10)*, 5491–5498.
[14] M. Iyanaga, Y. Aihara, N. Chatani, *J. Org. Chem.* **2014**, *79(24)*, 11933–11939.
[15] A. Pacheco-Benichou, T. Besson, C. Fruit, *Catalysts* **2020**, *10(5)*, 483.
[16] M. Fañanás-Mastral, *Synthesis* **2017**, *49(09)*, 1905–1930.
[17] K. Aradi, Á. Mészáros, B. L. Tóth, Z. Vincze, Z. Novák, *J. Org. Chem.* **2017**, *82(22)*, 11752–11764.
[18] A. Bigot, A. E. Williamson, M. J. Gaunt, *J. Am. Chem. Soc.* **2011**, *133(35)*, 13778–13781.
[19] M. Bouquin, F. Jaroschik, M. Taillefer, *Tetrahedron Lett.* **2021**, *75*, 153208.
[20] E. Cahard, H. P. J. Male, M. Tissot, M. J. Gaunt, *J. Am. Chem. Soc.* **2015**, *137(25)*, 7986–7989.
[21] X. Geng, S. Mao, L. Chen, J. Yu, J. Han, J. Hua, L. Wang, *Tetrahedron Lett.* **2014**, *55(29)*, 3856–3859.
[22] N. Gigant, L. Chausset-Boissarie, M.-C. Belhomme, T. Poisson, X. Pannecoucke, I. Gillaizeau, *Org. Lett.* **2013**, *15(2)*, 278–281.
[23] S.-H. Jung, D.-B. Sung, C.-H. Park, W.-S. Kim, *J. Org. Chem.* **2016**, *81(17)*, 7717–7724.
[24] S. Y. Moon, M. Koh, K. Rathwell, S.-H. Jung, W.-S. Kim, *Tetrahedron* **2015**, *71(10)*, 1566–1573.
[25] N. S. Soldatova, A. V. Semenov, K. K. Geyl, S. V. Baykov, A. A. Shetnev, A. S. Konstantinova, M. M. Korsakov, M. S. Yusubov, P. S. Postnikov, *Adv. Synth. Catal.* **2021**, *363(14)*, 3566–3576.
[26] S. G. Modha, M. F. Greaney, *J. Am. Chem. Soc.* **2015**, *137(4)*, 1416–1419.
[27] T. P. Lockhart, *J. Am. Chem. Soc.* **1983**, *105(7)*, 1940–1946.
[28] R. J. Phipps, N. P. Grimster, M. J. Gaunt, *J. Am. Chem. Soc.* **2008**, *130(26)*, 8172–8174.
[29] A. E. Allen, D. W. C. MacMillan, *J. Am. Chem. Soc.* **2011**, *133(12)*, 4260–4263.
[30] T. K. Stenczel, Á. Sinai, Z. Novák, A. Stirling, *Beilstein J. Org. Chem.* **2018**, *14*, 1743–1749.
[31] B. Chen, X.-L. Hou, Y.-X. Li, Y.-D. Wu, *J. Am. Chem. Soc.* **2011**, *133(20)*, 7668–7671.
[32] R. Sallio, P.-A. Payard, P. Pakulski, I. Diachenko, I. Fabre, S. Berteina-Raboin, C. Colas, I. Ciofini, L. Grimaud, I. Gillaizeau, *RSC Adv.* **2021**, *11(26)*, 15885–15889.

[33] N. Ichiishi, A. J. Canty, B. F. Yates, M. S. Sanford, *Org. Lett.* **2013**, *15(19)*, 5134–5137.
[34] N. Ichiishi, A. J. Canty, B. F. Yates, M. S. Sanford, *Organometallics* **2014**, *33(19)*, 5525–5534.
[35] T. L. Seidl, S. K. Sundalam, B. McCullough, D. R. Stuart, *J. Org. Chem.* **2016**, *81(5)*, 1998–2009.
[36] R. T. Gallagher, S. Basu, D. R. Stuart, *Adv. Synth. Catal.* **2020**, *362(2)*, 320–325.
[37] E. Lindstedt, M. Reitti, B. Olofsson, *J. Org. Chem.* **2017**, *82(22)*, 11909–11914.
[38] J. Malmgren, S. Santoro, N. Jalalian, F. Himo, B. Olofsson, *Chem. Eur. J.* **2013**, *19(31)*, 10334–10342.
[39] D. Koseki, E. Aoto, T. Shoji, K. Watanabe, Y. In, Y. Kita, T. Dohi, *Tetrahedron Lett.* **2019**, *60(18)*, 1281–1286.
[40] D. Sun, K. Yin, R. Zhang, *Chem. Commun.* **2018**, *54(11)*, 1335–1338.
[41] A. Nilova, B. Metze, D. R. Stuart, *Org. Lett.* **2021**, *23(12)*, 4813–4817.
[42] L. Neerbye Berntsen, A. Nova, D. S. Wragg, A. H. Sandtorv, *Org. Lett.* **2020**, *22(7)*, 2687–2691.
[43] R. Abha Saikia, D. Barman, A. Dutta, A. Jyoti Thakur, *Eur. J. Org. Chem.* **2021**, *2021(3)*, 400–410.
[44] R. A. Saikia, K. Talukdar, D. Pathak, B. Sarma, A. J. Thakur, *J. Org. Chem.* **2023**, *88(6)*, 3567-3581.
[45] S. Bhunia, G. G. Pawar, S. V. Kumar, Y. Jiang, D. Ma, *Angew. Chem. Int. Ed.* **2017**, *56(51)*, 16136–16179.
[46] Q. Yang, Y. Zhao, D. Ma, *Org. Process Res. Dev.* **2022**, *26(6)*, 1690–1750.
[47] C. Adamo, V. Barone, *J. Chem. Phys.* **1999**, *110(13)*, 6158–6170.
[48] S. Grimme, J. Antony, S. Ehrlich, H. Krieg, *J. Chem. Phys.* **2010**, *132(15)*, 154104.
[49] M. Cossi, N. Rega, G. Scalmani, V. Barone, *J. Comput. Chem.* **2003**, *24(6)*, 669–681.
[50] B. Modec, N. Podjed, N. Lah, *Molecules* **2020**, *25(7)*, 1573.
[51] M. J. Bausch, B. David, P. Dobrowolski, V. Prasad, *J. Org. Chem.* **1990**, *55(23)*, 5806–5808.
[52] L. Zhang, F. Zhou, Z. Li, B. Liu, R. Yan, J. Li, Y. Hu, C. Zhang, Z. Luo, K. Guo, *Polym. Chem.* **2020**, *11(35)*, 5669–5680.
[53] S. Kozuch, S. Shaik, *Acc. Chem. Res.* **2011**, *44(2)*, 101–110.
[54] R. Giri, J. F. Hartwig, *J. Am. Chem. Soc.* **2010**, *132(45)*, 15860–15863.
[55] T. L. Seidl, D. R. Stuart, *J. Org. Chem.* **2017**, *82(22)*, 11765–11771.
[56] K. Kepski, W. J. Moran, *Organics* **2022**, *3(3)*, 275–280.
[57] *Gaussian 16 Rev. C.01*, M. J. Frisch, G. W. Trucks, H. B. Schlegel, G. E. Scuseria, M. A. Robb, J. R. Cheeseman, G. Scalmani, V. Barone, G. A. Petersson, H. Nakatsuji, X. Li, M. Caricato, A. V. Marenich, J. Bloino, B. G. Janesko, R. Gomperts, B. Mennucci, H. P. Hratchian, J. V. Ortiz, A. F. Izmaylov, J. L. Sonnenberg, D. Williams-Young, F. Ding, F. Lipparini, F. Egidi, J. Goings, B. Peng, A. Petrone, T. Henderson, D. Ranasinghe, V. G. Zakrzewski, J. Gao, N. Rega, G. Zheng, W. Liang, M. Hada, M. Ehara, K. Toyota, R. Fukuda, J. Hasegawa, M. Ishida, T. Nakajima, Y. Honda, O. Kitao, H. Nakai, T. Vreven, K. Throssell, J. A. Montgomery, Jr., J. E. Peralta, F. Ogliaro, M. J. Bearpark, J. J. Heyd, E. N. Brothers, K. N. Kudin, V. N. Staroverov, T. A. Keith, R. Kobayashi, J. Normand, K. Raghavachari, A. P. Rendell, J. C. Burant, S. S. Iyengar, J. Tomasi, M. Cossi, J. M. Millam, M. Klene, C. Adamo, R. Cammi, J. W. Ochterski, R. L. Martin, K. Morokuma, O. Farkas, J. B. Foresman, and D. J. Fox, Gaussian, Inc., Wallingford CT, 2016.
[58] F. Weigend, *Phys. Chem. Chem. Phys.* **2006**, *8(9)*, 1057–1065.
[59] F. Weigend, R. Ahlrichs, *Phys. Chem. Chem. Phys.* **2005**, *7(18)*, 3297–3305.
[60] V. Barone, M. Cossi, *J. Phys. Chem. A* **1998**, *102(11)*, 1995–2001.

Manuscript received: August 22, 2023
Revised manuscript received: October 15, 2023
Accepted manuscript online: October 16, 2023
Version of record online: November 27, 2023